# Photogeneration of sound in a system of thermally insulated CdS microcrystals in zeolite

I. V. Blonskiĭ, M. S. Brodin, Yu. P. Piryatinskiĭ, G. M. Tel'biz,* V. A. Tkhorik, P. I. Tomchuk, and A. G. Filin

*Institute of Physics, Ukrainian Academy of Sciences, 252028 Kiev, Ukraine*
(Submitted 19 December 1994)
Zh. Éksp. Teor. Fiz. **107**, 1685–1697 (May 1995)

The nature of the photoacoustic response of CdS microcrystals synthesized in voids in zeolites was studied. Anomalously high sound-generation efficiency was observed, for the first time, in CdS/Y-zeolite samples irradiated with nanosecond laser pulses. A theory which takes into account the characteristics of the thermoelastic process in a system of thermally insulated semiconductor microcrystals was developed. The results of the investigations of photoacoustic spectra with harmonic modulation of the light flux as well as time-resolved photoluminescence spectra are presented. These results indicate that CdS percolation clusters are formed in Y-zeolite. © *1995 American Institute of Physics.*

## 1. INTRODUCTION

Among the many types of quantum-size semiconductors, the semiconductors in which migration of electronic excitations is limited in all three directions are of special interest. These media are called "quasi-zero-dimensional" or quantum currents. Promising models of quasi-zero-dimensional media, whose properties are now being actively studied,[1,2] are regular lattices of microcrystals of different semiconductor compounds synthesized in the voids of a zeolite matrix. Zeolites are complicated crystalline media which consist of alternating tetrahedral sublattices of the compounds $SiO_4$ and $AlO_4$ and have a hollow structure, similar to that of fullerene.[3] The diameter of the interior voids in the most common modifications of Y zeolite is 1.3 nm, which admits up to 11 CdS molecules per void. Because the $SiO_4$ and $AlO_4$ sublattices are joined along the network of oxygen atoms, the zeolite structure is also characterized by extended hollow channels with a diameter of 0.5 nm.[1] It is because zeolites contain characteristic pores of fixed size that such materials were chosen as a matrix for synthesizing clusters of different semiconductor compounds in the pores.[2] The scientific interest in such objects has been focused mainly on the possibility of the formation of a three-dimensional superlattice, the renormalization of the energy spectrum of charge carriers as a result of the quantum-size effect, and general questions concerning the theory of electronic spectra with a transition from a continuous medium into a quasidiscrete (molecular) state.[2]

In the present paper we call attention to another aspect of the problem of the fundamental properties of such materials—the characteristics of the energy-conversion processes in which electronic excitations of spatially separated thermally insulated CdS microcrystals participate. They are especially strongly manifested in the photoacoustic effect in the CdS/Y–zeolite samples which we investigated.

The crux of the photoacoustic effect is the generation of elastic waves in a medium irradiated with intensity-modulated light.[4] The effect is based on a chain of energy-conversion processes: absorption of light by the substance → pulsed heating → cooling → generation of elastic waves. We distinguish between gas-microphone detection of the signal, which yields information about the efficiency of the conversion of the absorbed light energy into thermal energy in the crystal,[5] and piezoelectric detection, which yields information about the conversion of absorbed energy into thermal energy and thermal energy into elastic energy of the lattice.[6]

## 2. EXPERIMENTAL PROCEDURE

Synthetic NaY zeolite was used as the starting material for preparing zeolites containing CdS microcrystals. Ion exchange was realized between sodium and cadmium ions as a result of a substitution reaction between NaY zeolite suspensions and a cadmium nitrate solution. After ion exchange, the cation-substituted zeolites were washed up to a negative reaction on $NO^-$, filtered, and dried. The reaction product obtained was subjected to thermovacuum treatment followed by sulfidization. After the samples were vaccum cooled, excess hydrogen sulfide was adsorbed. The specific technological conditions and a qualitative analysis of the samples investigated is described in detail in Ref. 7. Here, we merely note that the experimental samples were prepared in the form of $5\times5\times0.1$ mm$^3$ films with different molar weight $p$ of CdS in Y-zeolite: 2.76%, 11.22%, 11.66%, 13.45%, and 18.02%.

The photoacoustic response of the samples was investigated under excitation with short light pulses ($t=6$ ns) with a peak power of $10^5$ W from two laser sources: a nitrogren-vapor laser ($\lambda=337.1$ nm) and a tunable (over the range 580–680 nm) laser operating on 6-aminophenalenone in polyurethanecrylate. The photoacoustic signal was recorded with a specially constructed cell, consisting of a $20\times10\times1.5$ mm$^3$ sapphire acoustic line, at whose opposite ends the experimental sample and a TSTS-19 piezoelectric ceramic were attached along the large face. The details of this apparatus and the sinusoidally modulated photoacoustic spectrometer that we used are described in Ref. 8.

To perform fast diagnostics of the structural quality of the experimental samples, we also measured their time-

 1063-7761/95/050939-07$10.00  

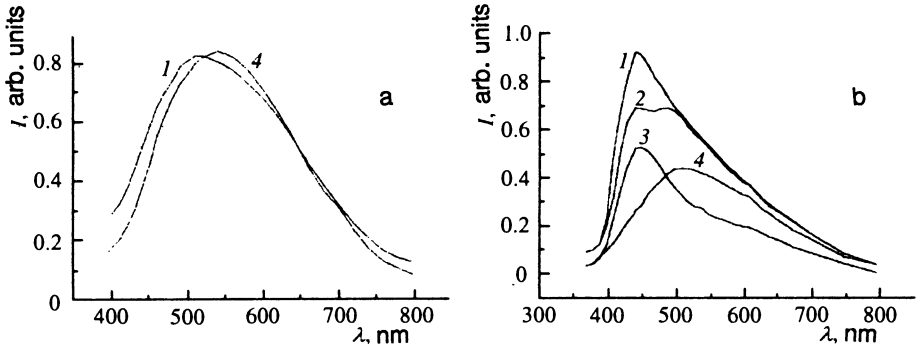


FIG. 1. Time-resolved photoluminescence spectra of group I (a) and II (b) CdS/Y-zeolite samples. The spectra were recorded at room temperature with different time delays $\tau$ measured from the maximum of the excitation pulse: $\tau = 1$ (*1*), 12 (*2*), −5 (*3*), and 22 (*4*) ns.

resolved photoluminescence spectra excited with a nitrogen-vapor laser. The layout of the luminescence apparatus is described in Ref. 9.

## 3. EXPERIMENTAL RESULTS

### 3.1. Time-resolved photoluminescence spectra

All experimental samples excited by the nitrogen-laser radiation at room temperature luminesce in the visible range of the spectrum. The structure of the emission spectrum and the kinetics of emission depend on the composition of the CdS/Y-zeolite system. For example, in samples with 11.22% CdS a wide emission band with a maximum at 520 nm is observed in the photoluminescence spectra. The maximum intensity in this band is achieved with a time delay of $\tau > 10$ ns (Fig. 1a). In addition to the band indicated above, another band with a maximum near 440 nm and a time delay of less than 10 ns is manifested in the spectra of the samples with the lowest CdS concentration ($p = 2.66\%$). The dynamics of the temporal evolution of the photoluminescence spectra of samples of this type is illustrated in Fig. 1b.

The results presented indicate that the CdS microcrystals in the experimental samples have different forms. We note that three of the most frequently encountered structural forms of CdS in Y-zeolite are distinguished.[1,2] At the lowest concentrations ($p < 1.1\%$), isolated semiconductor clusters less than 1.3 nm in size are usually formed. For such CdS/Y-zeolite samples, there is characteristically no luminescence, even at 4.2 K, and the fundamental absorption edge is shifted to 280 nm, which is associated with the manifestation of the quantum-size effect.[2] The second type of CdS structure in zeolite is a percolation clusters. Such clusters are formed by the merging of isolated clusters along hollow channels of the zeolite matrix with higher CdS concentrations in the zeolite. This structural form is, as a rule, characteristic of samples with initial CdS concentrations ranging from 1.1% to 10%. For samples of the second type, excitonic states near 350 nm are characteristically manifested in the absorption spectrum, and two bands with maxima at 440 and 520 nm also appear in the photoluminescence spectrum.[2] Finally, for even higher values of $p$, CdS microcrystals whose dimensions do not predetermine the appearance of quantum-size effects form outside the zeolite structure. Therefore, the edge absorption spectrum of samples of the third type is identical to the spectrum of bulk CdS single crystals, and the 520 nm band is the shortest-wavelength band in the luminescence spectrum.

In summary, it follows from the photoluminescence spectra presented in Fig. 1 and their interpretation from the standpoint of Refs. 1 and 2 that our experimental samples consisted of two structural forms of CdS in zeolite: percolation clusters ($p = 2.76\%$ CdS) and micron size CdS microcrystals outside the zeolite structure ($p > 11.22\%$).

For convenience, in what follows we divide our samples into two groups: group I contains samples with micron-size semiconductor microcrystals and group II contains samples with percolation clusters.

### 3.2. Photoacoustic response and its spectral dependence accompanying harmonic modulation of the light flux

Figure 2 displays the first measurements of the amplitude $U_{PA}$ of the photoacoustic response of samples from groups I and II. The measurements were performed at room temperature. The samples were irradiated with a DKsSH-500 xenon lamp. The radiation first passed through a large-aperture diffraction monochromator and were intensity-modulated at 75 Hz. The signal was recorded with a gas microphone. The photoacoustic cell employed consisted of an air-filled, hermetically sealed chamber with a quartz illuminator. The experimental sample and the microphone membrane were positioned inside the chamber.

As one can see from Fig. 2, the spectral characteristics of the photoacoustic response of the group I and II samples are substantially different. In group I samples, the spectral dependence $U_{PA}(\lambda)$ for $\lambda < 400$ nm saturates, while for group II samples $U_{PA}$ increases continuously as $\lambda$ decreases. To explain why the behavior of $U_{PA}$ ($\lambda$) for group I samples is different from that of group II samples, we shall consider the basic assumptions of the theory of the photoacoustic signal generated when semiconductor materials are excited by harmonically modulated light.[5,10] In the gas-microphone method that we used to measure the photoacoustic response, the variable component of the gas pressure on the microphone membrane is recorded. This component is directly proportional to the change in temperature on the irradiated surface of the experimental sample, and this change reflects the efficiency with which the absorbed light energy is converted into ther-

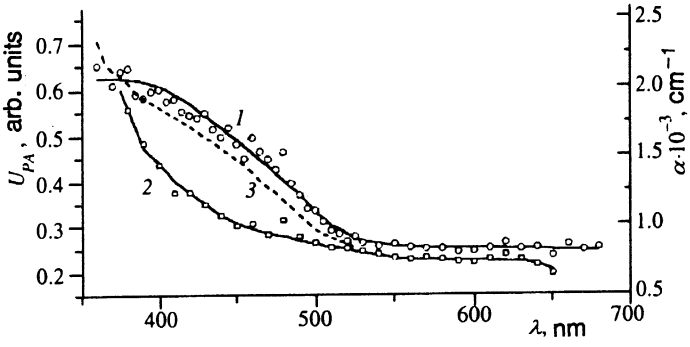


FIG. 2. Photoacoustic spectra for group I (*1*) and group II (2) CdS/Y-zeolite samples. The spectra were recorded with the light flux sinusoidally modulated at 75 Hz. Curve *3* represents the spectral distribution of the absorption coefficient according to Ref. 1.

mal energy. The quantity $U_{PA}$ is given by the following expression from Ref. 5:

$$U_{PA}=AI_0(\lambda)\alpha(\lambda)\eta(\lambda)[1-R(\lambda)]F,$$

where $A$ is a constant, determined by the structural characteristics of the gas-microphone cell; $\alpha(\lambda)$ is the spectral distribution of the absorption coefficient, $R(\lambda)$ is the spectral distribution of the reflection coefficient; $\eta(\lambda)$ describes the conversion efficiency of absorbed light energy into thermal energy of the lattice; and, $F$ is a complex function determined by the thermal and optical properties of the sample and the gas in the photoacoustic cell. The physical meaning of $U_{PA}$ can be appreciated by analyzing $F$, whose form depends on the ratios of the characteristic parameters $l_t$, $l_\alpha$, and the sample thickness $d$, where $l_t=(2\chi/\Omega)^{1/2}$ is the wavelength of the thermal wave and $l_\alpha=1/\alpha$ is the penetration depth of light in the material, $\chi$ is the thermal diffusivity of the experimental sample, and $\Omega=2\pi f$ is the angular frequency at which the light is modulated. When $l_t<l_\alpha<d$, $U_{PA}(\lambda)$ reflects the behavior of $U_{PA}(\lambda)$ mimics the function $\alpha(\lambda)$. For the opposite sense of the relationship between $l_t$ and $l_\alpha$, the function $U_{PA}(\lambda)$ is determined mainly by the thermal characteristics of the experimental samples and of the buffer gas in the gas-microphone cell. Taking this into consideration, the reasons why the behavior of $U_{PA}(\lambda)$ is different for samples in group I and II must be sought in the structural features of the experimental samples. As we have already mentioned, in analyzing the luminescence spectra, the technology used to prepare the group I samples presupposed the formation of a large number of micron-size CdS crystals. The absorption spectrum of this phase of CdS in Y-zeolite was first reconstructed in Ref. 2. This spectrum is represented by the dashed curve *3* in Fig. 2. It is interesting that in the spectral range 400–500 nm, the behavior of $\alpha(\lambda)$ is qualitatively the same as that of $U_{PA}(\lambda)$ for group I samples, and that at shorter wavelengths there is no such correlation. As far as group II samples are concerned, $\alpha(\lambda)$ and $U_{PA}(\lambda)$ are uncorrelated over the entire range of wavelengths $\lambda$. These results can be explained on the basis of the theory of Ref. 5 and model calculations, based on real parameters of CdS microcrystals.[11] In particular, it is shown in Ref. 11 that $l_t<l_\alpha$ for $\alpha<10^3$ cm$^{-1}$ and light-modulation frequency close to the frequency which we employed for CdS microcrystals. Therefore, for $\lambda>500$ nm, where $\alpha<10^3$ cm$^{-1}$, $U_{PA}(\lambda)$ reflects the spectral distribution of the absorption coefficient. For $\alpha>10^3$ cm$^{-1}$ we have $l_t>l_\alpha$, and thermal saturation obtains.

The preparation conditions of group II samples were such that percolation clusters with sizes suggesting manifestation of quantum size effects were obtained in a Y-zeolite matrix. The intrinsic edge absorption spectrum of CdS in such a structure is shifted 120 nm blueward with respect to bulk single crystals.[2] Therefore, $\alpha\ll 10^3$ cm$^{-1}$ in our range of $\lambda$ (350–700 nm); this suggests that the condition $l_t<l_\alpha$ is also satisfied. Therefore, $U_{PA}(\lambda)$ in group II samples reflects the light-absorption spectrum, except that now the spectrum is determined by the structural defects.

In concluding this section, we note that for comparison we performed similar measurements on CdS single-crystal plates grown by the method of gas-transport reactions. The qualitative spectral dependence $U_{PA}(\lambda)$ for these samples is illustrated by curve *1* in Fig. 2. However, the absolute value of $U_{PA}(\lambda)$ for single-crystal wafers was equal to about 1/20 of the value of the corresponding parameter for CdS/Y-zeolite samples. This indicates that the absorbed energy is converted more efficiently into thermal energy of the lattice in CdS microcrystals encapsulated into the zeolite matrix than CdS single-crystal wafers. This is most likely due to the structural features of CdS in zeolite, specifically, the highly extended surface of the microcrystals, as a result of which the contribution of surface recombination of nonequilibrium current carriers to the total heating of the sample is larger.

### 3.3. Photoacoustic response under pulsed excitation

Figure 3 displays the typical form of the pulsed photoacoustic response of our experimental samples under excitation with nanosecond laser pulses and with piezoelectric detection of the signal. The structure of the response is virtually identical for group I and II CdS/Y-zeolite samples and CdS single-crystal wafers with the same dimensions. We also did not observe any changes in the structure of the response at wavelengths in the range 337–650 nm. Only the signal amplitude changes. First, we shall discuss the structure of the response.

A general theory of the pulsed photoacoustic response of semiconductors was first described in Refs. 12 and 13. According to this theory, the bipolarity of an elementary pulse must be associated to the propagation of a stretching-compression wave in the sample, and the repeated acoustic "ringing" must be associated to the repeated reflection of the sound wave in the sample and the acoustic line as the wave propagates toward the piezoelectric transducer. The time delay of 2 $\mu$s in the oscillogram displayed in Fig. 3 is deter-

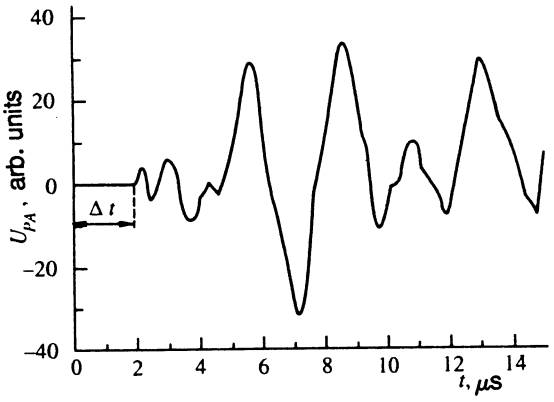


FIG. 3. Oscillogram of the pulsed photoacoustic response of the experimental samples in a cell with piezoelectric recording of the signal. The excitation source is a nitrogen-vapor laser ($\lambda$=337.1 nm) with a pulse duration of 6 ns.

mined by the sum of the characteristic times: the appearance time of sound in the photoexcited semiconductor and the propagation time of the elastic wave in the experimental sample, the acoustic line, and the piezoelectric transducer.

The basic result of this part of the paper follows from a comparison of the amplitudes of the pulsed photoacoustic response of CdS microcrystals encapsulated in the zeolite matrix and CdS single-crystal wafers. When the samples are excited in the region of the intrinsic interband absorption, the amplitude of the signal for group I CdS/Y-zeolite samples is more than ten times the corresponding parameter $U_{PA}$ for single-crystal CdS wafers. The amplitude of the photoacoustic response of group II samples is also much greater (by approximately a factor of five) than $U_{PA}$ for single-crystal wafers. When the samples are excited in the part of the spectrum where they are transparent (600 nm), $U_{PA}$ for CdS microcrystals in zeolite was also greater than the corresponding value for single-crystal wafers. This ratio of the amplitudes of the pulsed photoacoustic response for CdS microcrystals encapsulated in zeolite, on the one hand, and single-crystal CdS plates, on the other, was unexpected, since zeolite is a viscous material, and this, together with the lower volume density of CdS in zeolite, suggested a very low efficiency of sound generation in such a heterogeneous medium. To explain the results, we analyze the possible characteristics of sound generation in a system of thermally insulated microcrystals. In so doing, taking into consideration the experimentally observed fact that the CdS microcrystals are locally superheated, our analysis will focus on the thermoelastic mechanism.

## 4. THEORY OF SOUND GENERATION IN A SYSTEM OF THERMALLY INSULATED PHOTOEXCITED SEMICONDUCTOR MICROCRYSTALS AND DISCUSSION OF THE EXPERIMENTAL RESULTS

### 4.1. Initial assumptions of the theory

Consider a dielectric matrix, which contains inclusions in the form of spatially separated semiconductor microspheres with radius $a$. We assume that the band gap $E_g^i$ of the inclusions is smaller than the band gap $E_g^m$ of the matrix. Let the system be irradiated by a laser light flux of the form

$$I=I_0(r,\Omega)f(t). \tag{1}$$

Here, $f(t)$ is a modulation function, whose form will be specified below. We also assume that the energy of the exciting photon $h\nu$ falls in the range

$$E_g^i<h\nu<E_g^m, \tag{2}$$

which suggests excitation of only the intrinsic nonequilibrium current carriers of the semiconductor phase. We also take into consideration the experimental fact that recombination of the nonequilibrium current carriers in such structures, which have an extended surface, is mainly nonradiative. This should result, in turn, in significant superheating of such semiconductor inclusions, since it is assumed that the microcrystals are thermally insulated. Generally speaking, the superheating temperature of the electrons can be different from that of the lattice. However, since the temperature difference mentioned above can affect only times at most of the order of the electron energy relaxation time, we shall consider only the heating of the lattice of inclusions.

Partial heating of the matrix also gives rise to heating of the inclusions. The equation determining the temperature of an inclusion and the surrounding matrix has the standard form:

$$\frac{\partial}{\partial t}(CT)=\operatorname{div}(K\nabla T)+Q,$$
$$C=\begin{cases} C^{(i)}, & r<a, \\ C^{(m)}, & r>a, \end{cases} \quad K=\begin{cases} K^{(i)}, & r<a, \\ K^{(m)}, & r>a. \end{cases} \tag{3}$$

In Eq. (3) $C^{(i)}$ and $C^{(m)}$ are heat capacities; $K^{(i)}$ and $K^{(m)}$ are the thermal conductivities of the inclusions and the matrix, respectively, and $Q$ is the energy absorbed by an inclusion per unit time and per unit volume. On the basis of the inequalities (2), we can write

$$Q=\begin{cases} Q_0(t), & r<a, \\ 0, & r>a. \end{cases} \tag{4}$$

The energy absorbed by an inclusion per unit time depends on the magnitude of the flux $I$ and the absorption cross section $\sigma$:

$$VQ_0(t)=I\sigma. \tag{5}$$

We assume that the inclusions are small enough that the coordinate dependence of the temperature inside an inclusion can be neglected, i.e.,

$$\sqrt{\frac{\omega C}{K}}\,a\ll 1. \tag{6}$$

In other words, we assume that because an inclusion is small, the same temperature is established instantaneously throughout the volume $V$ of the inclusion. Then, integrating Eq. (3) over the volume of an inclusion (i.e., over $r$ in the range $0<r<a+\varepsilon$, $\varepsilon>0$) and Fourier transforming, we obtain

$$\left[-i\omega VC^{(i)}T(\omega)-K^{(m)}S\frac{\partial T}{\partial r}\right]_{r=a}=VQ_0(\omega), \tag{7}$$

where $S=4\pi a^2$ is the surface area of an inclusion. The inequality (6) will serve as the boundary condition for Eq. (3) in the region $r>a$.

The solution of Eq. (3) for $r>a$ (in the Fourier representation) has the form

$$T(r,\omega)=\frac{A}{r}\exp\left[-\sqrt{\frac{\omega C^{(m)}}{2K^{(m)}}}(1-i)r\right]. \tag{8}$$

We reckon the temperature everywhere relative to its value in the absence of the laser flux. Determining the constant $A$ in Eq. (7) from the boundary condition (6) and taking into consideration the inequality (8), we obtain

$$T(r,\omega)\approx\frac{VQ_0(\omega)}{4\pi aK^{(m)}}. \tag{9}$$

The solution (9) was written in a coordinate system whose origin lies at the center of an inclusion. As $r\to a$, we obtain from Eq. (9) the temperature of the inclusion, which, taking into account Eq. (6), assumes the form

$$T_i(t)\approx\frac{VQ_0(t)}{4\pi aK^{(m)}}=\frac{a^2Q_0(t)}{3K^{(m)}}. \tag{10}$$

### 4.2. Manifestation of the thermoelastic mechanism of sound generation in a system of thermally insulated semiconductor microcrystals

We shall now analyze the two terms that determine the manifestation of the thermoelastic mechanisms of sound generation in the experimental systems. The periodic change of the size of an inclusion gives rise to pulsations of the temperature of the inclusion in accordance with Eq. (10), i.e., it results in the generation of elastic waves propagating in the matrix. Under the action of the modulated laser flux, the radius of an inclusion oscillates according to the law

$$a=a_0+qT_i(t), \tag{11}$$

where $a_0$ is the equilibrium radius of an inclusion and $q$ is the linear expansion coefficient of an inclusion in the matrix.

The second mechanism is determined by the propagation of a residual heat wave in the matrix and by the effect of this wave on the components of the stress tensor of the matrix.

If the displacement vector for the longitudinal acoustic oscillations is represented in the form

$$\mathbf{u}_L=\nabla\Psi, \tag{12}$$

then the scalar function $\Psi$ satisfies the following equation (see, for example, Ref. 14):

$$\nabla^2\Psi-\frac{1}{c_L^2}\frac{\partial^2\Psi}{\partial t^2}=\frac{k\beta}{c_L^2g}T(t). \tag{13}$$

Here, $c_L$ is the propagation velocity of longitudinal acoustic waves, $k$ is the bulk modulus, $\beta$ is the thermal expansion coefficient of the matrix, and $g$ is the density of the matrix.

Equation (13) refers to the case of a single inclusion in the matrix. In what follows, we shall consider the aggregate effect of many inclusions.

The solution of the homogeneous equation corresponding to Eq. (13), satisfying the boundary condition

$$\left(\mathbf{u}_L\frac{\mathbf{r}}{r}\right)\Big|_{r=a}=\frac{\partial\Psi}{\partial r}\Big|_{r=a}=qT_i(t), \tag{14}$$

describes the first of the above-mentioned mechanisms of sound generation, and the particular solution of the inhomogeneous Eq. (13) describes the second mechanism.

The solution of the homogeneous equation corresponding to Eq. (13) and satisfying the condition (14) has the form[14]

$$\Psi_0(r,t)=-\frac{qc_La}{r}\exp\left[-\frac{c_L}{a}\left(t-\frac{r-a}{c_L}\right)\right]\times\int_{-\infty}^{t-(r-a)/c_L}d\tau\exp\left(\frac{c_L\tau}{a}T_i\right)(\tau). \tag{15}$$

At large distances from the inclusion ($r\gg a$, the far-field picture) and at low modulation frequencies of the light flux ($\Omega<c_L/a$) the solution (15) simplifies:

$$\Psi_0(r,t)=-\frac{qa^2}{r}T_i\left(t-\frac{r}{c_L}\right). \tag{16}$$

Substituting into Eq. (16) $T_i$ from Eq. (10), we obtain

$$\Psi_0(r,t)=-\frac{qa^4Q_0(t-r/c_L)}{3K^{(m)}r}. \tag{17}$$

The expression (17) determines the contribution of a separate inclusion to the generation of longitudinal acoustic waves (determined by the pulsation of the sizes of the inclusions) at large distances from an inclusion.

The particular solution of the inhomogeneous equation (13) in the Fourier representation is

$$\Psi_n(\mathbf{r},\omega)=\frac{k\beta}{c_L^3g}\int\frac{d\mathbf{r}'}{|\mathbf{r}-\mathbf{r}'|}T(\mathbf{r}',\omega)\exp\left(i\frac{\omega}{c_L}|\mathbf{r}-\mathbf{r}'|\right). \tag{18}$$

As follows from Eq. (9), $T(r,\omega)$ changes considerably over distances of the order of

$$r_0\approx\sqrt{\frac{2K^{(m)}}{\omega C^{(m)}}}\sqrt{\frac{2\chi}{\omega}}.$$

For large distances from an inclusion ($r>r_0$), which correspond to the experimentally realizable regime of signal detection by a piezoelectric transducer, the integrand in Eq. (18) can be expanded in powers of $r'$ and the integration can be performed. The result is

$$\Psi_n(r,\omega)=\frac{VQ_0(\omega)k\beta}{K^{(m)}gc_L^2}\frac{\chi}{\omega}\frac{ic_L^2+\omega\chi}{c_L^4+(\omega\chi)^2}\frac{\exp(i\omega r/c_L)}{r}. \tag{19}$$

We found a solution of Eq. (13) in the form of a sum of two terms [see Eqs. (17) and (19)] without specifying thus far the modulation function in Eq. (1).

To find $Q_0(\omega)$ using the expression (5), the form of the modulation function $f(t)$ must now be specified. For generality, it is useful to consider two limiting cases of modulation: continuous modulation (low frequency $\Omega$) and "modulation" with a $\delta$-function pulse or a series of such pulses separated by long intervals.

We assume that $f(t)$ in Eq. (1) has the form

$$f(t)=\begin{cases} 1+\cos(\Omega t), & \text{(20a)} \\ \delta(t). & \text{(20b)} \end{cases}$$

In accordance with Eq. (5) as well as Eqs. (20a) and (20b), we find

$$VQ_0(\omega)=\begin{cases} \pi\sigma I_0[\delta(\omega-\Omega)+\delta(\omega+\Omega)], & \text{(21a)} \\ \sigma I_0. & \text{(21b)} \end{cases}$$

For the case of harmonic modulation, in accordance with Eqs. (21a) and (19), we obtain

$$\Psi_n(r,t)=\frac{\sigma I_0 k\beta}{K^{(m)}gc_L^2}\frac{\chi}{\Omega}\,\mathrm{Re}\,\frac{ic_L^2+\Omega\chi}{c_L^4+(\Omega\chi)^2}\frac{\exp[-i\Omega(t-r/c_L)]}{r}$$
$$=\frac{\sigma I_0 k\beta}{K^{(m)}gc_L^2}\frac{\chi}{\Omega}\frac{\cos[\Omega(t-r/c_L)-\varphi(\Omega)]}{r}. \qquad (22)$$

In Eq. (22) the phase $\varphi(\Omega)$ is determined by the relation

$$\cot[\varphi(\Omega)]=\frac{\chi\Omega}{c_L^2}. \qquad (23)$$

Using Eqs. (19) and (21b), we obtain for a single $\delta$-function laser pulse

$$\Psi_n(r,t)=\frac{\sigma I_0 k\beta}{K^{(m)}gc_L^2}\frac{1}{r}\int_0^\infty\frac{d\omega}{(c_L^4+(\omega\chi)^2)\omega}$$
$$\times\left\{\chi\omega\cos\left[\left(t-\frac{r}{c_L}\right)\omega\right]+c_L^2\sin\left[\left(t-\frac{r}{c_L}\right)\omega\right]\right\}$$
$$=\frac{\sigma I_0 k\beta}{K^{(m)}gc_L^2}\frac{1}{r}\int_0^\infty\frac{d\omega}{\omega}\cos\left[\left(t-\frac{r}{c_L}\right)\omega-\varphi(\Omega)\right]. \qquad (24)$$

It follows from Eq. (24) that in this case the heat wave arising in the matrix generates an entire packet of acoustic waves, mainly at low frequencies $\omega<c_L^2/\chi$.

Equations (17), (22), and (24) describe the generation of waves by an isolated inclusion. When there are many such inclusions, in Eqs. (17), (22), and (24) $\mathbf{r}$ must be replaced by $|\mathbf{r}-\mathbf{r}_j|$ and the summation must extend over all inclusions, whose centers are now determined by the vector $\mathbf{r}_j$. In addition, the intensity of the laser flux must also be taken at the point $\mathbf{r}_j$.

If, for example, a cylindrically symmetric laser beam is incident on a semiconductor plate perpendicular to the surface of the wafer, then the laser intensity at the point $\mathbf{r}_j$ can be expressed as

$$I_0(\mathbf{r}_j)=I_0\exp\left(-\alpha z_j-\left(\frac{\zeta_j}{\zeta_0}\right)^2\right). \qquad (25)$$

Here, $\zeta_0$ is the characteristic size of the beam. The laser symmetry axis points along the $z$ axis.

In the case of continuous modulation of the laser beam, in accordance with Eq. (22), we have in the presence of many inclusions

$$\Psi_n(\mathbf{r},t)=\frac{\sigma I_0 k\beta}{K^{(m)}gc_L^2}\frac{\chi}{\Omega}\sum_j\exp\left\{-\alpha z_j-\frac{\zeta_j^2}{\zeta_0^2}\right\}$$
$$\times\frac{\cos[\Omega(t-|\mathbf{r}-\mathbf{r}_j|/c_L)]-\varphi(\Omega)}{|\mathbf{r}-\mathbf{r}_j|}. \qquad (26)$$

In this formula $\mathbf{r}_j=\zeta_j+\mathbf{k}_0 z_j$ and $\mathbf{r}=\zeta+\mathbf{k}_0 z$, where $\mathbf{k}_0$ is the unit vector in the $z$ direction. The general formula (26) can be greatly simplified in different specific situations. For example, if the point of observation of the acoustic waves is chosen so that

$$\zeta\gg\zeta_0,\min(d,1/\alpha), \qquad (27)$$

then it follows from Eq. (26), under the condition (27), that

$$\Psi_n(\mathbf{r},t)=\frac{\sigma I_0 k\beta}{K^{(m)}gc_L^2}\frac{\chi}{\Omega}NV_0\frac{\cos[\Omega(t-\zeta/c_L)-\varphi(\Omega)]}{|\zeta|}. \qquad (28)$$

In Eq. (28) $N$ is the concentration of inclusions and $V_0$ is the volume equal to the product of the cross-sectional area of the laser beam and the lesser of $d$ and $1/\alpha$.

In the case of a $\delta$-function laser pulse and under the condition (27), the acoustic signal produced by the pulsation of the sizes of the inclusions assumes the form, in accordance with Eq. (17),

$$\Psi_0(\mathbf{r},t)=-\frac{qa^4NV_0I_0\delta(t-\zeta/c_L)}{3K^m\zeta}. \qquad (29)$$

If terms of order $\zeta_0/\zeta$ are taken into account, then the $\delta$-function will be smeared. In Eqs. (28) and (29) we do not take into account the possible "ringing" associated with repeated reflections of sound from the walls of the matrix.

In the case of a $\delta$-function laser pulse and sound excitation by the heat wave it generates in the matrix, as one can see from Eq. (24), the acoustic spectrum will be quite wide and it will be concentrated in the frequency range $\omega<c_L^2/\chi$.

In summary, our theoretical analysis of the experimental data shows that a system of spatially separated, thermally insulated, semiconductor microcrystals, an example of which is "CdS-zeolite," is an effective medium for photogeneration of sound. As follows from Eq. (26), in such media the spectral composition of the sound waves can be changed by choosing materials with suitable thermal and elastic characteristics as well as by varying the sizes of the microcrystals. The main reason for the high efficiency of sound generation in a heterogeneous medium consisting of a matrix with low thermal conductivity and thermally conducting semiconductor microcrystals as inclusions is the strong pulsed superheating of the microcrystals. Moreover, as shown in Ref. 15, in a piezoelectric semiconductor with above-threshold free-electron velocities, sound dissipation can be reversed, which will greatly intensify the effect. The experimental data obtained from investigations of the dependence of the intensity

and spectral composition of the sound waves on the sizes of the crystallites in the system "CdS—zeolite" will be presented in a separate paper.

## 5. CONCLUSIONS

In the present paper we presented the results of experimental investigations of the time-resolved photoluminescence spectra, photoacoustic spectra with harmonic modulation of the exciting radiation, and pulsed photoacoustic response of CdS microcrystals encapsulated in a zeolite matrix. It was shown that under the influence of photoexcitation, the efficiency with which the absorbed energy is converted into thermal energy and thermal energy is converted into the elastic energy of the lattice in a system of thermally insulated semiconductor microcrystals is orders of magnitude higher than for bulk single crystals. This may be of practical interest. A theory of the thermoelastic mechanism of sound generation in a system of thermally insulated, spatially separated microcrystals, which takes into account the local superheating of the microcrystals, was developed to give a qualitative explanation of the results obtained. To make a strict quantitative comparison between the experimental and theoretical results, other mechanisms of sound generation, primarily the electron-deformation and striction mechanisms, a systematic theory of which does not now exist, must be taken into account.

Financial support for this work was provided by the GKNT Foundation for Fundamental Research of Ukraine.

*Institute of Physical Chemistry, Ukrainian Academy of Sciences, 252039 Kiev, Ukraine.

[1] Y. Wong and N. Herron, J. Phys. Chem. **91**, 257 (1987).
[2] Y. Wong and N. Herron, J. Phys. Chem. **98**, 4988 (1988).
[3] S. V. Kozyrev and V. V. Rotkin, Fiz. Tekh. Poluprovodn. **27**, 1409 (1993) [Sov. Phys. Semicond. **27**, 777 (1993)].
[4] V. P. Zharov and V. S. Letokhov, *Laser Optoacoustic Spectroscopy* [in Russian], Nauka, Moscow, (1984) [Springer-Verlag, New York (1986)].
[5] A. Rosencwaig and A. Gersho, J. Appl. Phys. **46**, 64 (1976).
[6] Yu. V. Gulyaev, A. I. Morozov, and V. Yu. Raevskiĭ, Akust. Zh. **31**, 469 (1985) [Sov. Phys. Acoust. **31**, 278 (1985)].
[7] G. M. Telbiz, V. M. Gunko, and G. Tamulajtis, React. Kinet. Catal. Lett. **50**, 215 (1993).
[8] I. V. Blonskij, V. G. Grytz, and V. A. Tkhoryk, SPIE Proc. **2113**, 1001 (1994).
[9] M. S. Brodin, I. V. Blonskiĭ, and V. V. Tishchenko, Pis'ma Zh. Éksp. Teor. Fiz. **32**, 119 (1980) [JETP Lett. **32**, 108 (1980)].
[10] V. A. Sablikov and V. B. Sandomirskiĭ, Fiz. Tekh. Poluprovodn. **17**, 81 (1983) [Sov. Phys. Semicond. **17**, 50 (1983)].
[11] T. Arai, T. Yoshida, and T. Ogawa, Jpn. J. Appl. Phys. **26**, 396 (1983).
[12] V. E. Gusev and A. A. Karabutov, *Laser Optoacoustics* [in Russian], Nauka, Moscow (1991) [American Institute of Physics, New York (1993)].
[13] S. A. Akhmanov and V. E. Gusev, Usp. Fiz. Nauk **162**, 3 (1992) [Sov. Phys. Usp. **35**, 153 (1992)].
[14] P. M. Tomchuk, Ukr. Fiz. Zh. **38**, 1174 (1993).
[15] J. W. Tucker and V. W. Rampton, *Microwave Ultrasonics in Solid State Physics*, North-Holland, Amsterdam (1973).

Translated by M. E. Alferieff